N78-24054

SOME MEASUREMENTS OF AN EBF POWERED-LIFT WAKE

William G. Johnson, Jr.
NASA Langley Research Center

SUMMARY

This paper discusses a summary of the analysis of results from a wind-tunnel investigation in which velocity vector measurements were obtained in the near wake of an externally blown flap powered-lift configuration. These measurements were used to develop spanwise distributions for the momentum strength and location of the engine exhaust stream tube with the results used as input parameters to one jet-flap analytical method.

This analysis showed that a comparison of the momentum coefficients obtained from forward speed wake surveys with the predicted values from static force data results in a good correlation, which verifies the use of the flap thrust recovery factor as a means of predicting the momentum strength at the flap trailing edge. Also, when wake survey distributions of momentum strength and direction are used as input parameters to one analytical jet-flap method, the results show reasonable agreement between the experimental data and analytical results.

INTRODUCTION

Powered lift is now being examined for application to conventional long-haul transports in order to enhance their take-off and landing performance as well as for short or reduced take-off and landing aircraft. To assist in the design of these aircraft, various analytical methods have been devised to predict the behavior of thick jet-flap powered-lift wakes. Experience has shown that these methods depend significantly on the descriptions of the wake momentum strength and location which are used as input parameters.

This paper will discuss a summary of the analysis of results from a wind-tunnel investigation (ref. 1) in which velocity vector measurements were obtained in the near wake of an externally blown flap powered-lift configuration. These measurements were then used to develop spanwise distributions for the momentum strength and location of the engine exhaust stream tube with the results used as input parameters to one jet-flap analytical method.

8

SYMBOLS

b wing span, m

c wing chord, m

C_L lift coefficient, $\frac{\text{Lift}}{q_\infty S}$

C_T thrust coefficient, $\frac{\text{Gross static thrust}}{q_\infty S}$

$C_\mu{}^*$ section momentum coefficient from wake surveys

C_μ total momentum coefficient from wake surveys

n number of velocity vectors in jet thickness

q_∞ free-stream dynamic pressure, Pa

S wing area, m^2

V magnitude of velocity vector, m/sec

V_j magnitude of specific velocity vector associated with $\delta_{j,l}$, m/sec

V_∞ free-stream velocity, m/sec

y distance along span of wing, m

α angle of attack, deg

δ_f flap deflection, deg

δ_j jet deflection angle, $\arctan \frac{\text{Normal force}}{\text{Axial force}}$, deg

$\delta_{j,l}$ local downwash angle minus wing angle of attack, deg

$\delta_j{}^*$ mean turning angle at any given survey station, deg

$\Delta\delta_j{}^*$ change in turning angle due to power, deg

η flap thrust recovery, $\frac{\text{Resultant force}}{\text{Static thrust}}$

τ jet thickness

DISCUSSION

The investigation was conducted in the Langley V/STOL tunnel on an existing externally blown flap model (ref. 2). As shown in figure 1, measurements were made at 11 spanwise stations between the edge of the fuselage and the

midsemispan station on the wing. The measurements were made with a split-film total vector anemometer which was capable of sensing the three velocity vector components (ref. 3). At each spanwise station, the probe was moved through a vertical arc through the wake and measured more than 100 velocity vectors at each survey station for each engine-power-off and engine-power-on condition.

Figure 2 shows a sample of the power-on velocity profiles taken at zero angle of attack and for thrust coefficients of 2.0 and 4.0. The profiles are shown at the two spanwise stations, $\frac{y}{b/2} = 0.227$ and $\frac{y}{b/2} = 0.376$, which are just inboard of the engine center lines. The outline of the wing-flap system is shown to locate the profiles relative to the 35° deflected flap and engine thrust center line. Units of free-stream velocity are indicated by dashed arcs within the profile. The profiles show higher than free-stream velocity flow above the wing and lower than free-stream velocity flow below the engine exhaust stream tube. The planform sketch in figure 1 shows that at the inboard station, the flap trailing edge is at a greater distance from the engine exhaust plane than at the outboard station. This greater distance results in the inboard exhaust stream tube being more diffuse than the jet sheet wake at the outboard station. Figure 2 shows that this wake characteristic holds for both thrust levels.

To establish the vertical bounds of the engine exhaust stream tube, a jet thickness τ was defined as the wake region in which the change in the local velocity vectors exceeded 0.3 m/sec. The magnitudes of the velocity vectors within the jet thickness were integrated to obtain a section momentum coefficient $C_\mu{}^*$ at each spanwise station by the following equation:

$$C_\mu{}^* = \frac{\int_0^\tau \left(V_{\text{power on}}\right)^2 d\tau - \int_0^\tau \left(V_{\text{power off}}\right)^2 d\tau}{\frac{1}{2} V_\infty{}^2 c}$$

This equation provides for the subtraction of the power-off momentum from the power-on momentum in coefficient form per unit area. The results of this integration are shown in figure 3 as a function of the spanwise location $\frac{y}{b/2}$. The data show that the peaks of the distributions have shifted significantly inboard of the engine center lines. This shift is contrary to the accepted thought that the engine exhaust spreads significantly outboard on a swept-wing configuration.

In addition to obtaining values for the distribution of the momentum strength and location along the flap trailing edge for analytical purposes, a comparison of a total momentum coefficient due to power from the forward speed-wake surveys and the predicted momentum coefficient obtained by use of static force data would be useful in verifying the technique generally used for defining the strength of engine exhaust momentum at the flap trailing edge. To obtain the wake survey value, the section momentum coefficient distributions were extrapolated to the edge of the fuselage $\left(\frac{y}{b/2} = 0.126\right)$ and to the most outboard extent

of the wing felt to be impacted by the spread engine exhaust flow $\left(\frac{y}{b/2} = 0.6\right)$. The distributions were then integrated spanwise to obtain the total momentum coefficient C_μ due to the engine exhaust at the flap trailing edge. The predicted value from static force data is obtained from the product of the static parameter η and the engine thrust coefficient C_T, where η is defined as the efficiency of turning the engine exhaust flow through some deflection angle. When the static force data are plotted as shown in figure 4, the value of η can be obtained as the radial distance from the origin to the data point. A comparison of the integrated values of engine momentum coefficient from the forward speed wake surveys with the product of the static values of η and C_T is shown in figure 5, and the result is a very good agreement for all of the thrust levels and angles of attack tested.

A mean turning angle $\delta_j{}^*$ was determined for each spanwise survey station by the following equation:

$$\delta_j{}^* = \frac{\sum_1^n V_j \delta_{j,l}}{\sum_1^n V_j}$$

where $\delta_{j,l}$ is the local downwash angle minus the wing angle of attack, V_j is the magnitude of the corresponding streamwise velocity vector, and n is the number of measured velocity vectors between the chosen limits. This equation weights $\delta_{j,l}$ by the velocity magnitude since it was felt that the higher velocity vectors had a stronger influence on the overall turning angle of the jet. The procedure was applied to the power-off and power-on data, with the resulting spanwise distributions shown in figure 6 by the circles and squares, respectively. These distributions show a change in the peak locations from those in the momentum distributions - the peaks are now shown on the engine center lines. This characteristic indicates that for this configuration $\left(\delta_f = 35^o\right)$, most of the engine exhaust is passing under the flap trailing edge with little turning. Since most jet-flap theories use the description of the jet-wake effects as an addition to basic wing theory, the local flow angle due to power was obtained by subtracting the power-off distributions from the power-on distributions. The results are shown in figure 7 as a function of spanwise station.

The distributions which were obtained for the momentum coefficients (fig. 3) and jet-deflection angles (fig. 7) were then used as input parameters to a jet-flap analytical method developed by Lissaman (ref. 4). The results of the computation are compared in figure 8 with the experimental lift coefficients as a function of wing angle of attack. The comparison indicates analytical results similar to the corresponding experimental data.

CONCLUSIONS

The analysis of results from a survey of the near wake of an externally blown flap configuration has resulted in the following conclusions:

1. A comparison of the momentum coefficients obtained from forward speed wake surveys with the predicted values from static force data results in a good correlation, which verifies the use of the flap thrust recovery factor as a means of predicting the momentum strength at the flap trailing edge.

2. When wake survey distributions of momentum strength and direction are used as input parameters to one analytical jet-flap method, the results show reasonable agreement between the experimental data and analytical results.

REFERENCES

1. Johnson, William G., Jr.; and Kardas, Gerald E.: A Wind-Tunnel Investigation of the Wake Near the Trailing Edge of a Deflected Externally Blown Flap. NASA TM X-3079, 1974.

2. Johnson, William G., Jr.: Aerodynamic Characteristics of a Powered, Externally Blown Flap STOL Transport Model With Two Engine Simulator Sizes. NASA TN D-8057, 1975.

3. Olin, J. G.; and Kiland, R. S.: Split-Film Anemometer Sensors for Three-Directional Velocity-Vector Measurements. Aircraft Wake Turbulence and Its Detection, John H. Olsen, Arnold Goldburg, and Milton Rogers, eds., Plenum Press, Inc., 1971, pp. 57-79.

4. Lissaman, Peter B. S.: Analysis of High-Aspect-Ratio Jet-Flap Wings of Arbitrary Geometry. NASA CR-2179, 1973.

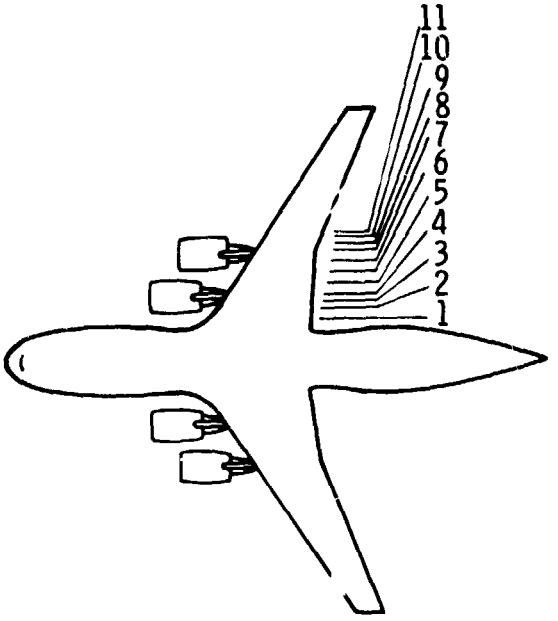

Figure 1.- Spanwise survey stations.

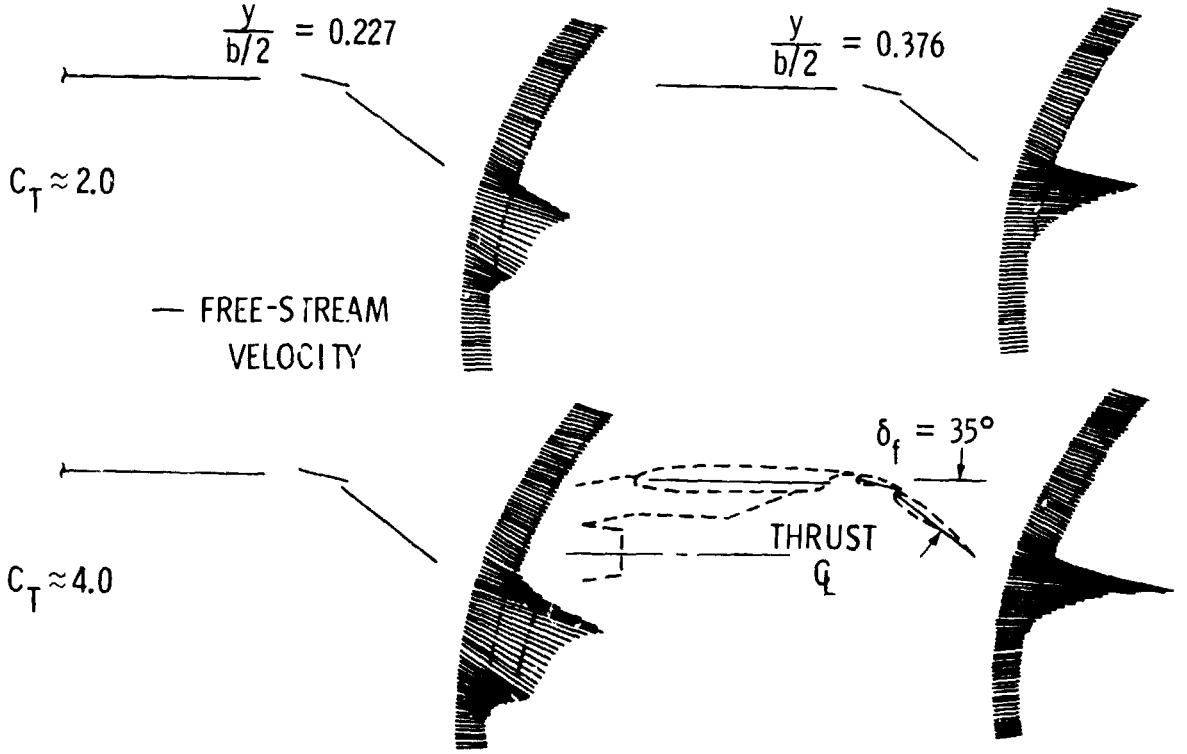

Figure 2.- Streamwise velocity profiles. $\alpha = 0^o$; $V_\infty = 25.45$ m/sec.

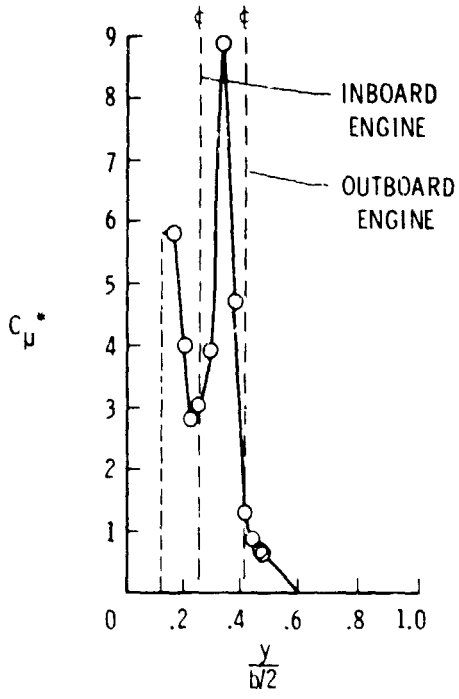

Figure 3.- Experimental momentum coefficient distribution. $\alpha = 0^\circ$; $C_T \approx 2.0$.

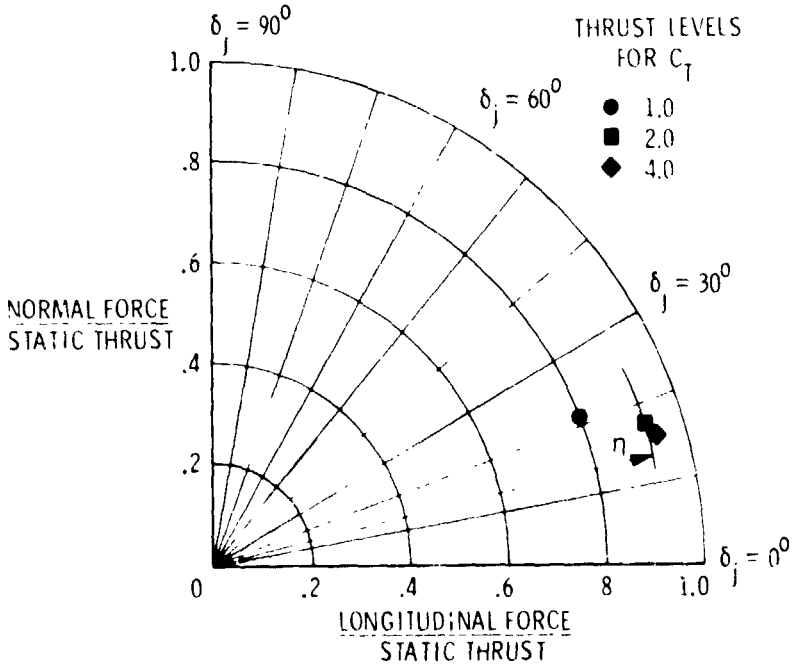

Figure 4.- Static turning angles and thrust recovery factor.

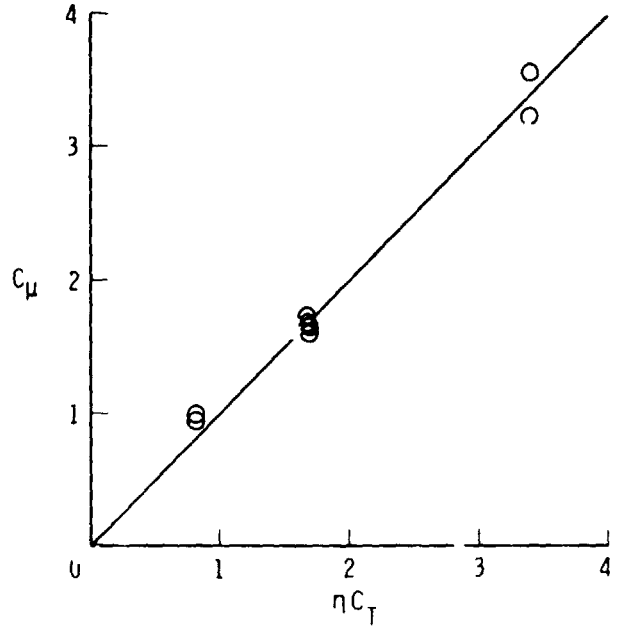

Figure 5.- Momentum coefficient from forward speed and static data.

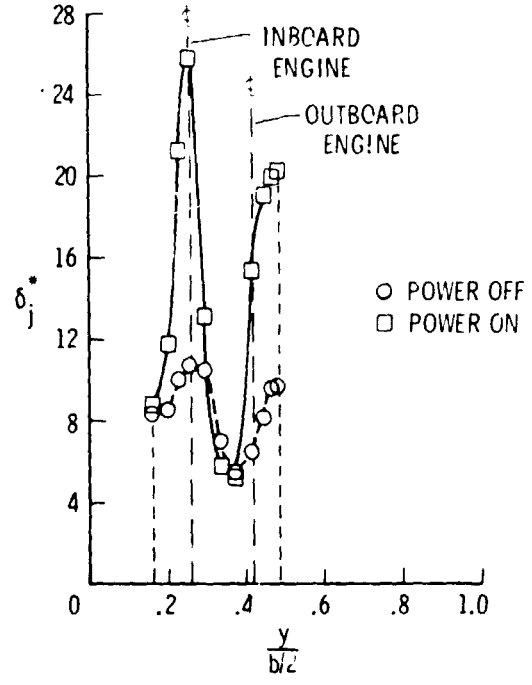

Figure 6.- Experimental distribution of jet-deflection angle. $\alpha = 0^o$; $C_T \approx 2.0$.

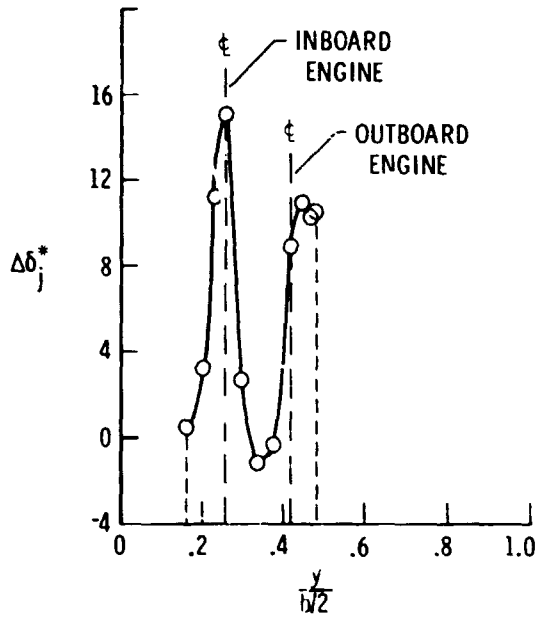

Figure 7.- Experimental jet-deflection angle due to power.
$\alpha = 0^\circ$; $C_T \approx 2.0$.

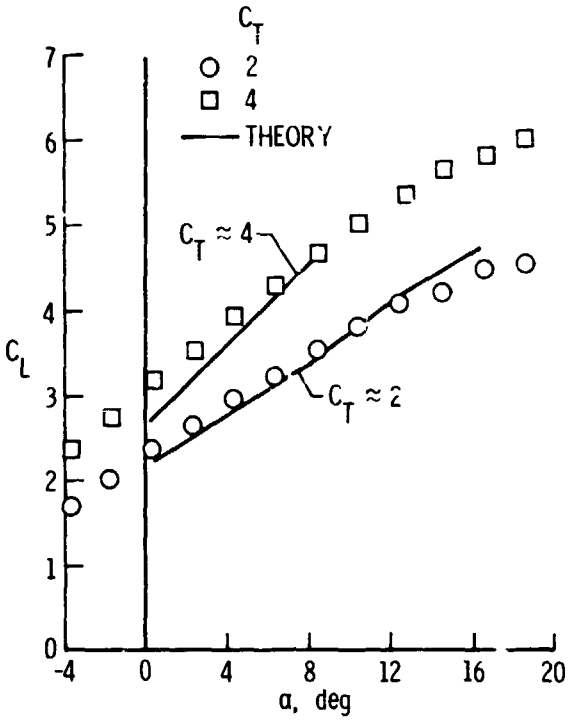

Figure 8.- Comparison of theory with experimental data for lift coefficient.